Characterization and RST control of a nonlinear piezoelectric actuator for a robotic hand

Sofiane Khadraoui *and **Micky Rakotondrabe** **

* *University of Sharjah, United Arab Emirates.*
** *LGP laboratory, National School of Engineering in Tarbes (ENIT-INPT), University of Toulouse, Tarbes France.*

(corresponding author: sofiane.khadraoui@gmail.com)

Abstract: This paper presents the characterization, modeling, and control of piezoelectric actuators of a robotic system by considering the temperature effect. Besides the sensitivity to temperature variation, quite often the behavior of piezoelectric actuators is negatively affected by badly-damped vibrations and nonlinear phenomena such as strong hysteresis and creep. An analysis of the sensitivity of piezoelectric actuators to temperature variations (thermo-mechanical displacement) is first presented and the characterization results are discussed. The effect of the temperature mainly on the hysteresis loops, the creep, and vibrations is presented. Then, a temperature-dependent model of piezoelectric actuators is derived based on the study and characterization results obtained. Finally, the model of piezoelectric actuators obtained is used to design a robust RST (Regulation-Sensitivity-Tracking) controller to improve their behavior and achieve a good quality of positioning tasks. Experimental validation is given to demonstrate the efficacy of the presented modeling and control methods.

Keywords: Characterization, Modeling, Temperature effect, Hysteresis, Creep, Vibration, Piezoelectric actuator, RST controller.

1. INTRODUCTION

The past few decades have been witnessed by considerable interest in the development of devices and technologies for precise positioning. In particular, piezoelectric actuators based devices are becoming increasingly important and attractive in a wide range of precise positioning applications where very high accuracy and resolution are required. Piezoelectric actuators applications mainly include hard disk drive [1], medical microrobots [2], dental machines [3], diesel engine injectors [4], scanning probe microscopes [5], microgripper [6], or robotic hands [7]. The wide range of piezoelectric actuators applications is mainly due to their appealing properties such as: 1) actuators do not have moving parts or exhibit friction; 2) high resolution because of their ability to provide motion in the sub-nanometer range; 3) large actuating force and high bandwidth; and 4) their relatively small size and easy physical integration. Considering all the aforementioned properties, we aim, within the French ECOSYSPRO project, at developing a robotic hand based on piezoelectric actuators capable of effectively manipulating high end pieces of pottery in automated carving and painting tasks. Such robotic hand, which is utilized as an end-effector of a parallel Delta-robot, consists of three piezoelectric actuators equally spaced on the surface of an equilateral triangular prism and are spaced 120^o apart as shown in Fig 1-a. The parallel Delta-robot is used to realize long-distance pick and place tasks, while the piezoelectric robotic hand is intended to perform both carving and painting tasks with a high precision better than $5\mu m$ so that high-end art objects are successfully produced. Beside their advantages outlined above, piezoelectric actuators suffers from some inherent issues such as hysteretic behavior and creep phenomenon. Moreover, beyond these characterestics, the hysteresis loops are very sensitive to the surrounding temperature variations [8]. Temperature effect on piezoelectric structures has been

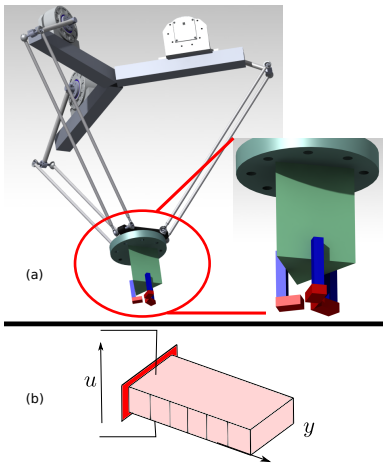

Fig. 1. (a): parallel robot and robotic hand with three piezoelectric actuators. (b): piezoelectric actuator.

⋆ This work is supported by the national CPER ECOSYSPRO project.

exploited to design a hybrid thermal piezoelectric actuator in [9] but this remains exceptional and cannot be applied to robotic hand which is devoted to handle sensitive objects. Thus, the general effect of temperature on piezoelectric actuator for robotic hand has to be considered as disturbance rather than advantage. It is well known that all the above complex characteristics (hysteresis, creep, temperature effect) of piezoelectric actuators degrade the performance of the tasks performed and cause undesirable vibrations or instability. These properties may negatively affect the quality of the objects carving and painting. As a conclusion, suitable control techniques, for piezoelectric actuators used in high precision applications, are needed to overcome the above problem. Several methods for the control of piezoelectric actuators, including feedforward and feedback schemes, have been reported in the literature. The feedforward control scheme has been applied to deal with the creep phenomenon [10], the inherent hysteresis nonlinearity [11, 12, 13], and the vibrations [14], independently. Other related works based on the feedforward control architecture considered all phenomena simultaneously by cascading the individual controllers [15, 16]. Generally, feedforward control scheme has many features such as the low cost and the high integration, however, its lack of robustness does not makes it suitable for the studied robotic system. This is mainly due to the fact that studied robotic system is subject to different disturbances caused by the carving task and the manipulated objects, which are of different types and shapes and act as a disturbance when interacting with the actuators. For this reason, several works using feedback control architecture have been proposed: experimental/analytical tuning of PID feedback controller for piezoelectric actuators[17], adaptive control method [18], sliding mode and backstepping control techniques [19] and robust control approaches including position positive feedback approach [20], H_∞ and interval-based control [21, 22, 23, 24].

The works above propose to reach the desired performances and to ensure robustness against possible uncertainties and possible external disturbances. Meanwhile, when all the phenomena (hysteresis, creep and oscillations) act together, the robustness is reduced and the loss of performances or even the stability is observed. In this paper, we are interested in the modeling and control of the piezoelectric actuator under these phenomena all together observed. Moreover, the actuator will work in an environment where the temperature varies. More precisely, the to be manipulated pieces and pottery are assumed to be at "high" temperature since either they come from precedent process of fabrication or they are subjected to process (laser or other kinds) while being kept by the robotic hand. This temperature variation strongly affect the piezoelectric actuator behavior and thus its performances to handle the pieces. In this paper therefore, we propose to design a control law robust enough to keep certain performances while rejecting the effects of temperature variation and of the above actuator properties.

The paper is organized as follows. In section-2, we characterize first the effect of the temperature variation on the piezoelectric actuator behavior after which we propose a model of the latter. Section-3 is devoted to the controller design and the resulting experimental aplication. Finally, conclusion and perspectives are presented in section-4.

2. THERMAL EFFECT ANALYSIS AND MODELING

The piezoelectric actuator we study is a piezoelectric stack as displayed in Fig 1-b. Its input is the driving voltage u and the output is the displacement y

2.1 Analysis

First, we analyze the effect of a varying ambient temperature on the actuator output displacement. Fig 2-a shows the evolution of the temperature T that we imposed to vary from 28^o to 45^o, and then to decrease back to 28^o. As shown in Fig 2-b (blue), the displacement y drifts from its initial value. Then the drift is slew down like a saturation even if the temperature continues to increase. Fig 2-b (red and black) show the same result but when the voltage applied to the actuator is not zero. Overall, from these results, the temperature introduces a drift of the actuator displacement until saturation. From the time domain results of Fig 2-a and -b, the temperature-displacement map is plotted. Fig 2-c gives the results which reveals that the thermal behavior of the actuator is hysteresis.

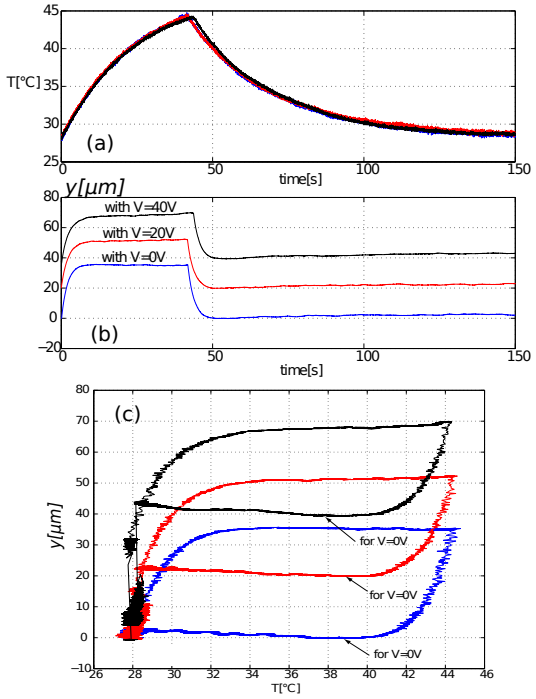

Fig. 2. (a): the applied temperature. (b): drift of the displacement. (c): displacement versus temperature .

Certain piezoelectric actuators conspicuously exhibits hysteresis and creep nonlinearities between the driving voltage and their output displacements. Let us check now the effects of the temperature on these phenomena. For the hysteresis, we applied a sine voltage $u(t)$ to the actuator. Then, after recording the resulting output displacement y, we plot the input-output map. Fig 3-a show the obtained curves obtained at four different frequencies. For each frequency used, we also subject the actuator to two different

temperatures. As from the results, the hysteresis characteristics of the actuator is not significantly affected by the temperature. To characterize the creep phenomenon, a step voltage is applied. It is defined as a slow displacement drift appearing after the transient part when a step voltage is applied to the actuator. According to the characterization reported in Fig 3-c, this creep phenomenon is higher when the actuator is under higher ambient temperature.

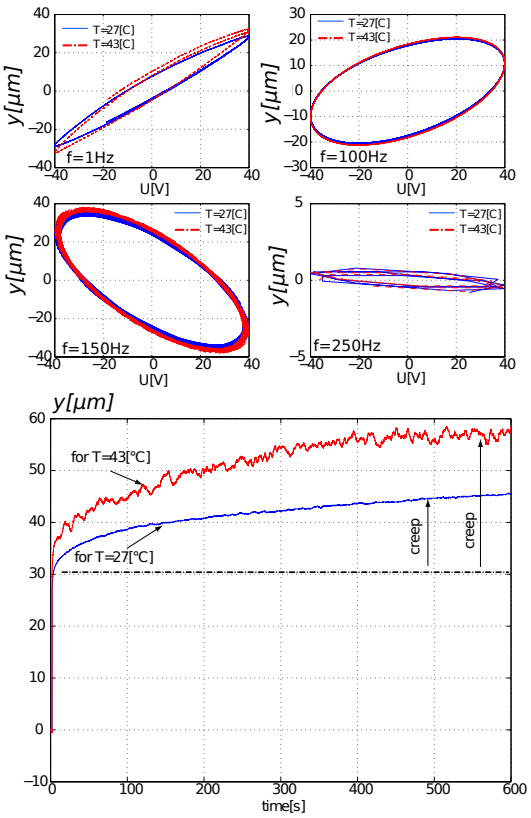

Fig. 3. Effect of the temperature on the hysteresis (a) and on the creep (b) curves.

The last verification deals with the dynamics of the actuator when applying a voltage. Fig 4-a presents the response of the actuator to a step voltage when it is subjected to two different temperatures. From the figure, it is approximately observed that the effect of the temperature on the step response is negligible. For more precision, a harmonic analysis was performed. Fig 4-b shows the resulting magnitude which confirms the low effect of the temperature on the dynamics of the actuator. The figure indicates that the (slight) difference is observed at low frequency which corresponds to creep phenomenon and possibly to hysteresis.

2.2 Modeling

To model the actuator behavior by considering the creep and the temperature effect, we consider the structure proposed in [25]:

$$y(t) = \Gamma_d\left(u(t)\right) + y_c(t) + y_T(t) \tag{1}$$

where $\Gamma_d\left(u(t)\right)$ is a nonlinear operator that represents the rate-dependent hysteresis of Fig 3-a, $y_c(t)$ is the additional drift observed in Fig 3-b and $y_T(t)$ is all additional displacement caused by the temperature.

Using the Hammerstein architecture to approximate the rate dependent-hysteresis $\Gamma_d\left(u(t)\right)$, and employing a Bouc-Wen approach for the resulting rate-independent hysteresis [25], $\Gamma_d\left(u(t)\right)$ can be replaced with $D(s)(u(s) - h(s))$ where $h(s)$ is the internal state of hysteresis, and $D(s)$ is a transfer function representing the dynamics to be identified. Considering $y_c(t)$ and $y_T(t)$ as output disturbance that one can translate to input disturbance u_c and u_T by transformation [25], we obtain:

$$y(s) = D(s)(u(s) - h(s) + u_c(s) + u_T(s)) \tag{2}$$

Thus, the final model becomes:

$$y(s) = D(s)(u(s) + d(s)) \tag{3}$$

where $d(s) = -h(s) + u_c(s) + u_T(s)$ is the input disturbance.

Using the experimental transient part in Fig 4-a and ARMAX (autoregressive–moving-average model with exogenous inputs) method of identification with Matlab, we obtained:

$$D(s) = \frac{107(s^2 + 1.4 \times 10^4 s + 6.1 \times 10^7)}{(s + 651)(s^2 + 42s + 1.5 \times 10^7)} \tag{4}$$

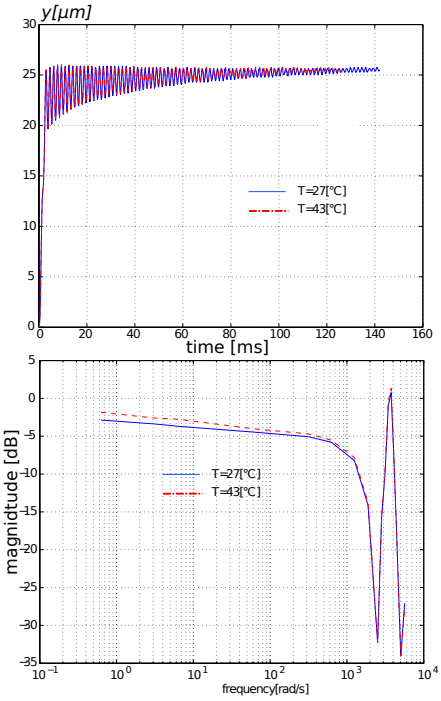

Fig. 4. Effect of the temperature on the dynamics.

Fig 5 presents the comparison between the simulation of the above identified model and the experimental step response. It shows that the identified model is precise enough for further controller design.

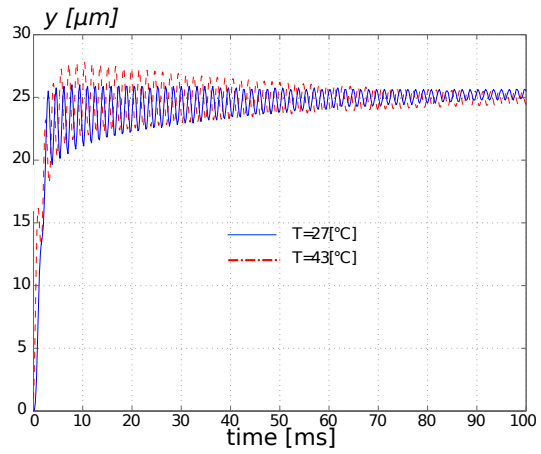

Fig. 5. Transient part: simulation and experimental result.

3. ROBUST RST CONTROL OF THE PIEZOCANTILEVER

In this section, we attempt to design an RST structured feedback controller for piezoelectric actuators represented mathematically by the Hammerstein architecture given in Subsection 2.2. The canonical structure of the RST control is a two degree of freedom control based on three polynomials, namely $R(s)$, $S(s)$, and $T(s)$, as shown in Fig 6. y_r, y, and u are the reference input, displacement of the piezoelectric actuator, and the input voltage, respectively. d is the total disturbance acting on the actuator that is assumed to include the effect of the creep, temperature variations effects, vibrations. It should be mentioned that RST controllers were originally designed in z-domain, however, without loss of generality, we aim here to design them in Laplace domain. Consider the linear dynamics of

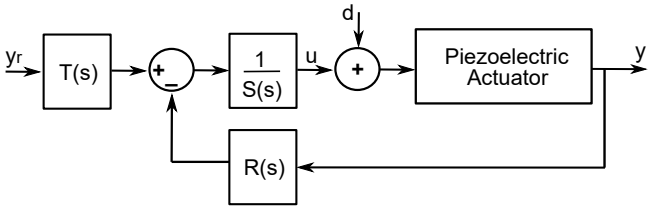

Fig. 6. RST feedback controller architecture.

the piezoelectric actuator defined by the following transfer function:

$$D(s) = \frac{B(s)}{A(s)} = \frac{b_m s^m + b_{m-1}s^{m-1} + \cdots + b_1 s + b_0}{s^n + a_{n-1}s^{n-1} + \cdots + a_1 s + a_0} \quad (5)$$

where $A(s)$ and $B(s)$ are co-prime polynomials of degrees n and m, respectively, such that $n \geq m$. $A(s)$ is monic. From the closed-loop system of Fig 6-b, the displacement of the piezoelectric actuator can be expressed as

$$y(s) = \frac{B(s)T(s)}{A(s)S(s) + B(s)R(s)} y_r + \frac{B(s)S(s)}{A(s)S(s) + B(s)R(s)} d \quad (6)$$

The RST controller polynomials have the following form:

$$\begin{aligned} R(s) &= \alpha_r s^r + \alpha_{r-1}s^{r-1} + \cdots + \alpha_1 s + \alpha_0 \\ S(s) &= s^k + \beta_{k-1}s^{k-1} + \cdots + \beta_1 s + \beta_0 \\ T(s) &= \gamma_p s^p + \gamma_{p-1}s^{p-1} + \cdots + \gamma_1 s + \gamma_0 \end{aligned} \quad (7)$$

where α's, β's, and γ's are the RST controller parameters. $S(s)$ is selected to be a monic polynomial. To ensure the causality of the RST controller, $r \leq k$ and $p \leq k$. Here, the following condition is used:

$$r = k \quad (8)$$

The key question is to tune the RST controller parameters so that satisfactory performance and robustness against the disturbance d are achieved. Generally, the closed-loop system stability and regulation performance can be improved using the polynomials $R(s)$ and $S(s)$, while a good tracking performance is ensured by a suitable selection of all polynomials. To enhance the capability of RST structure controller in terms of disturbance rejection and reference tracking, the loop transfer function should involve at least one integrator, i.e. polynomial $S(s)$ should contain at least one root at the origin. This fact makes the weight of d in (6) very small, and hence, it allows rejection of low frequency disturbances. In this paper, the disturbance d is mainly due to errors related to hysteresis and creep effects and temperature variations that are supposed to be significant in the low frequency range only. Hence, let us consider that $S(s)$ has one root at the origin, i.e. $\beta_0 = 0$, and hence $S(s)$ becomes:

$$S(s) = s^k + \beta_{k-1}s^{k-1} + \cdots + \beta_1 s$$

One possible solution to the control design problem outlined above is based on the idea of adjusting the closed-loop system setpoint response according to a desired closed-loop response defined by a reference model. This is known as the pole placement method which is based on solving the so-called Diophantine equation [26, 27]. It can be seen from (6) that the closed-loop system zeros are the zeros of $B(s)$ and those of the feedforward part $T(s)$ used to compensate the static gain and ensure a zero steady-state error. The closed-loop system poles are roots of the characteristic equation below:

$$\Delta(s) = A(s)S(s) + B(s)R(s) = 0$$

The reference model, which can be selected from the desired closed-loop performance specifications, is expressed as:

$$H^*(s) = \frac{B_m(s)}{A_m(s)} = \frac{B(s)B_{m_{\text{aux}}}(s)}{A_{m_{\text{dom}}}(s)A_{m_{\text{aux}}}(s)} \quad (9)$$

where

$$\begin{aligned} A_m(s) &= s^\delta + p_{\delta-1}s^{\delta-1} + \cdots + p_1 s + p_0 \\ B_m(s) &= l_\rho s^\rho + l_{\rho-1}s^{\rho-1} + \cdots + l_1 s + l_0 \end{aligned}$$

where p's and l's are the coefficients of the polynomials $A_m(s)$ and $B_m(s)$ respectively. $A_m(s)$ is monic and $\delta = n+k$ so that a solution of the Diophantine equation can be found as detailed below, while $\rho = m+p$. Generally, $A_m(s)$ can be factorized as $A_m(s) = A_{m_{\text{dom}}}(s)A_{m_{\text{aux}}}(s)$. $A_{m_{\text{dom}}}(s)$ is desired characteristic polynomial which specifies the desired location of the closed-loop system dominant poles, for which both stability and performance are ensured, while $A_{m_{\text{aux}}}(s)$ is an auxiliary polynomial with faster poles (at least 10 times smaller than the dominant poles) used to add a certain number of degrees of freedom. The polynomial $B_m(s)$ is supposed to contain the zeros of the system (roots of $B(s)$) and other zeros introduced to have more degrees of freedom in the tuning process. Hence, it can be factorized as $B_m(s) = B(s)B_{m_{\text{aux}}}(s)$. $B_{m_{\text{aux}}}(s)$ can be selected as a low-order polynomial with zeros located the farthest possible to the left in the complex plane (relative to the dominant poles). The objective is to make the closed-loop system behaves as the reference model (9).

Hence, the problem above can be solved by equating the actual closed-loop transfer function (from y_r to y) to the reference model as follows [27]:

$$\frac{B(s)T(s)}{A(s)S(s)+B(s)R(s)} = \frac{B_m(s)}{A_m(s)} = \frac{B(s)B_{m_{\text{aux}}}(s)}{A_{m_{\text{dom}}}(s)A_{m_{\text{aux}}}(s)} \tag{10}$$

which is reduced to

$$\frac{T(s)}{A(s)S(s)+B(s)R(s)} = \frac{B_{m_{\text{aux}}}(s)}{A_{m_{\text{dom}}}(s)A_{m_{\text{aux}}}(s)} \tag{11}$$

To ensure the desired dynamical behavior of the closed-loop system, one can solve Diophantine equation:

$$A(s)S(s)+B(s)R(s) = A_{m_{\text{dom}}}(s)A_{m_{\text{aux}}}(s) \tag{12}$$

The order of the desired characterestic polynomial should be equal to $\delta = n+k$ (order of $A(s)$ + order of $S(s)$). This allows the derivation of $n+k$ equations by equating the coefficients of identical powers of both sides of Diophantine equation. Moreover, Diophantine equation above involved $k-1$ unknown coefficients in $S(s)$ and $r+1 = k+1$ other unknowns in $R(s)$ (according to (8)), which makes a total of $2k$ unknows. To solve the $n+k$ equations for the unknowns, the order k of the polynomial $S(s)$ should satisfy the following condition:

$$n+k = 2k \implies k = n$$

Hence, updating the order of polynomials $R(s)$, $S(s)$ and $A_m(s)$ results in:

$$\begin{aligned} R(s) &= \alpha_n s^n + \alpha_{n-1}s^{n-1} + \cdots + \alpha_1 s + \alpha_0 \\ S(s) &= \beta_n s^n + \beta_{n-1}s^{n-1} + \cdots + \beta_1 s \\ A_m(s) &= A_{m_{\text{dom}}}A_{m_{\text{aux}}} = s^{2n} + p_{2n-1}s^{2n-1} + \cdots + p_0 \end{aligned} \tag{13}$$

Considering the fact that order of $A_m(s) = A_{m_{\text{dom}}}(s)A_{m_{\text{aux}}}(s)$ is $2n$, one can select the order of both polynomials $A_{m_{\text{dom}}}(s)$ and $A_{m_{\text{aux}}}(s)$ to be n. Using Equations (11) and (12), one can select $T(s) = B_{m_{\text{aux}}}(s)$, such that $T(0) = B_{m_{\text{aux}}}(0) = R(0)$ to achieve zero steady-state error (unit static gain of the closed-loop system). This leads to $\gamma_0 = l_0 = \alpha_0$.

3.1 Experimental results

The above controller has been applied to the piezoelectric actuator by using the scheme in Fig 6. Then the closed-loop was characterized experimentally.

First, we apply a step reference input displacement $y_r = 20\mu m$ to the closed-loop. After the output y reaches the reference, we vary the ambient temperature from 28^o to almost 45^o and then back to 30^o as displayed in Fig 7-a. From Fig 7-b, the output displacement is not at all influenced by the temperature variation and remains equal to the reference.

In order to evaluate the dynamics of the closed-loop, we zoomed on the transient part of the step response of the system to an input of $10\mu m$. Fig 8-a shows the result which indicates good performances: the oscillations of the natural system (see Fig 4-a) are removed, the statical error is almost zero. In Fig 8-b is shown the harmonic response of the system which confirms the removal of the peak. The step response and the harmonic response were carried out at two different temperatures and the results show (see the figures) that the performances remain the same,

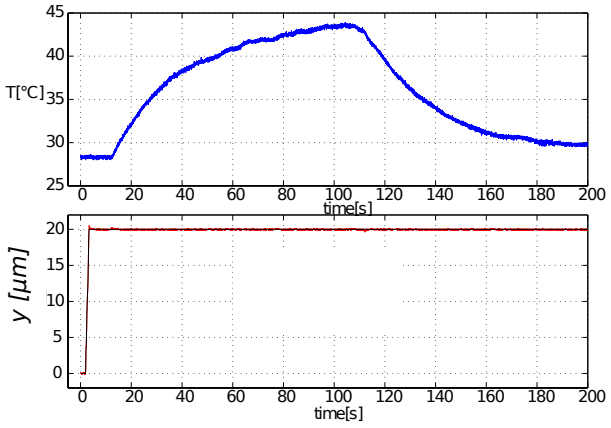

Fig. 7. Rejection of the drift due to temperature variation.

which demonstrates the efficiency of the controller to reject temperature effects.

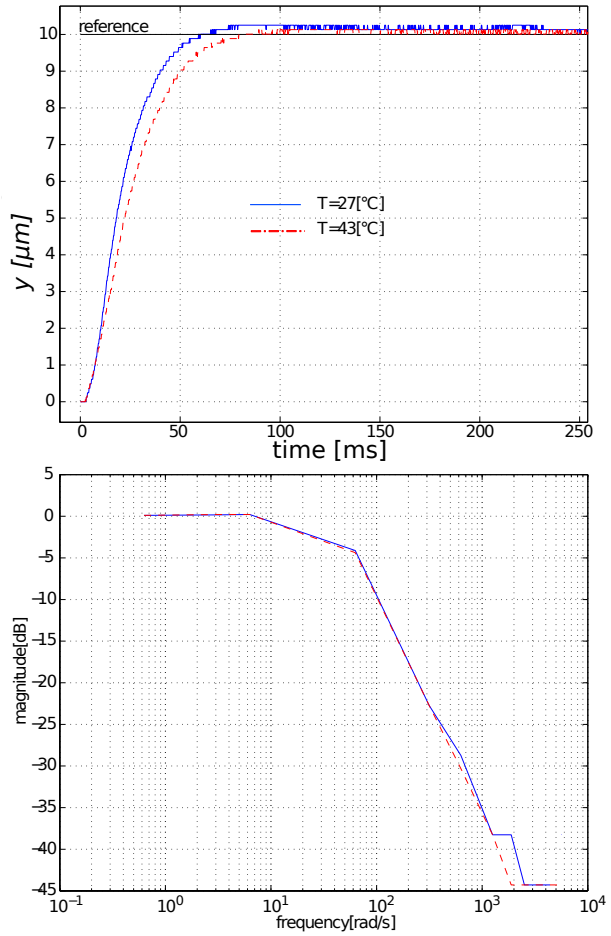

Fig. 8. (a) step response. (b) harmonic response.

4. CONCLUSION

The paper presented the characterization, modeling and control of a piezoelectric actuator for robotic hand for working in environment with varying temperature. The characterization shown that for a given voltage, the output displacement of the actuator is strongly affected and modified by the temperature when the latter varies. We also

concluded that while the hysteresis and the dynamics characteristics of the actuator were not significantly affected by the temperature, the creep phenomenon was strongly affected. We therefore proposed to model the actuator by considering the temperature effect and by lumping it, along with the creep and the hysteresis terms, in an input disturbance. Then, we proposed to use a robust RST controller that showed both performance improvement and disturbance rejection capabilities. Experiments on the real system were carried out and demonstrated the efficiency of the controller to maintain the same performance despite the temperature variation. The feedback control was performed using an external sensor. However, the sensor itself can be affected by temperature variation as well. Moreover, within a robotic hand, implementing such external sensor will be a challenge. As an alternative to this, we propose to study in the future the self-sensing method. It will consist in using the same piezoelectric actuator as its proper sensor. To this, we will study and extend the previous work [28, 29] in order to account and thus to reject the temperature effect in the self-sensing measurement.

REFERENCES

[1] S Kon et al. Design and fabrication of a piezoelectric instrumented suspension for hard disk drives. In *Smart Structures and Materials*, volume 6174, pages 951–960, 2006.

[2] L Mattos et al. μralp and beyond: Micro-technologies and systems for robot-assisted endoscopic laser microsurgery. *Frontiers in Robotics and AI*, 2021.

[3] D Deepa et al. Piezosurgery in dentistry. *Journal of Oral Research and Review*, 8(1):27, 2016.

[4] F Salvador et al. Complete modelling of a piezo actuator last-generation injector for diesel injection systems. *Int Journal of Engine Research*, 15(1), 2012.

[5] G Binnig et al. Atomic force microscope. *Physical review letters*, 56(9):930–933, 1986.

[6] S Khadraoui et al. Optimal design of piezoelectric cantilevered actuators with guaranteed performances by using interval techniques. *IEEE/ASME Trans on Mechatronics*, 19(5), 2013.

[7] G Flores and M Rakotondrabe. Robust nonlinear control for a piezoelectric actuator in a robotic hand using only position measurements. *IEEE Control Systems Letters*, 6:872–877, 2021.

[8] M Al Janaideh et al. On hysteresis modeling of a piezoelectric precise positioning system under variable temperature. *Mechanical Systems and Signal Processing*, 145:106880, 2020.

[9] M Rakotondrabe and A Ivan. Development and dynamic modeling of a new hybrid thermopiezoelectric microactuator. *IEEE/ASME Trans on Mechatronics*, 26(6), 2010.

[10] M Rakotondrabe. Modeling and compensation of multivariable creep in multi-dof piezoelectric actuators. In *IEEE Int Conf on Robotics and Automation*, pages 4577–4581, 2012.

[11] D Habinez et al. Multivariable generalized bouc-wen modeling, identification and feedforward control and its application to multi-dof piezoelectric actuators. In *IFAC WC*, pages 10952–10958, 2014.

[12] M Rakotondrabe. Multivariable classical prandtl–ishlinskii hysteresis modeling and compensation and sensorless control of a nonlinear 2-dof piezoactuator. *Nonlinear Dynamics*, 89(1):481–499, 2017.

[13] R Oubellil et al. Experimental model inverse-based hysteresis compensation on a piezoelectric actuator. In *Int Conf on System Theory, Control and Computing*, pages 186–191. IEEE, 2015.

[14] D Croft and S Devasia. Vibration compensation for high speed scanning tunneling microscopy. *Review of Scientific Instruments*, 70(12):4600–4605, 1999.

[15] D Croft et al. Creep, hysteresis, and vibration compensation for piezoactuators: atomic force microscopy application. *J. Dyn. Sys., Meas., Control*.

[16] D Habineza et al. Multivariable compensation of hysteresis, creep, badly damped vibration, and cross couplings in multiaxes piezoelectric actuators. *IEEE Trans on Automation Science and Eng*, 15(4), 2018.

[17] A Youssef. Optimized pid tracking controller for piezoelectric hysteretic actuator model. *World Journal of Modelling and Simulation*, 9(3):223–234, 2013.

[18] Y-T Liu et al. Model reference adaptive control for a piezo-positioning system. *Precision engineering*, 34(1):62–69, 2010.

[19] J-A Escareno et al. Backstepping-based robust-adaptive control of a nonlinear 2-dof piezoactuator. *Control Engineering Practice*, 41:57–71, 2015.

[20] J Ling et al. A robust resonant controller for high-speed scanning of nanopositioners: design and implementation. *IEEE Trans on Control Systems Technology*, 28(3):1116–1123, 2019.

[21] H Ladjal et al. H_∞ robustification control of existing piezoelectric-stack actuated nanomanipulators. In *IEEE Inter Conf on Robotics and Automation*, pages 3353–3358, 2009.

[22] M Rakotondrabe. Performances inclusion for stable interval systems. In *American Control Conference*, pages 4367–4372, 2011.

[23] S Khadraoui et al. Combining h_∞ approach and interval tools to design a low order and robust controller for systems with parametric uncertainties: application to piezoelectric actuators. *International Journal of control*, 85(3):251–259, 2012.

[24] M Hammouche et al. Robust and guaranteed output-feedback force control of piezoelectric actuator under temperature variation and input constraints. *Asian Journal of Control*, 22(6):2242–2253, 2020.

[25] M Rakotondrabe. Piezoelectric systems for precise and high dynamic positioning: design, modeling, estimation and control. *Habilitation, Univ of Franche-Comté*, 2014.

[26] K Astrom and B Wittenmark. *Computer controlled systems: theory and design*. Englewood Ciffs, NJ: Prentice-Hall, 1996.

[27] K Astrom and B Wittenmark. *Adaptive control*. Dover Publications, Inc., New York, 2013.

[28] M Rakotondrabe. Combining self-sensing with an unkown-input-observer to estimate the displacement, the force and the state in piezoelectric cantilevered actuator. In *American Control Conf*, pages 4523–4530,, 2013.

[29] I Ivan et al. Quasi-static displacement self-sensing measurement for a 2-dof piezoelectric cantilevered actuator. *IEEE Trans on Indus Elec*, 64(8), 2017.